Hydrogen abstraction from methane on a magnesia (001) surface

ARTICLE *in* THE JOURNAL OF PHYSICAL CHEMISTRY · SEPTEMBER 1991

Impact Factor: 2.78 · DOI: 10.1021/j100172a053

2 AUTHORS, INCLUDING:

Lars G M Pettersson
Stockholm University
318 PUBLICATIONS **10,891** CITATIONS

SEE PROFILE

Hydrogen Abstraction from Methane on an MgO(001) Surface

Knut J. Børve† and Lars G. M. Pettersson*

Institute of Theoretical Physics, University of Stockholm, Vanadisvägen 9, S-113 46 Stockholm, Sweden
(Received: November 26, 1990)

Hydrogen abstraction from methane over the pure and doped MgO(001) crystal surface has been studied at the SCF, CASSCF, and multireference CI levels by use of a cluster model combined with the surface Madelung potential. Li and Na as dopants stabilize a reactive O^- state at the surface and give abstraction reactions with low barrier (4–6 kcal/mol). Second-layer Mg and Mg^+ vacancies also result in a low barrier, but somewhat endothermic reactions. Be and Mg stabilize O^{2-}, which is very unreactive toward hydrogen abstraction. This is in agreement with experimental evidence indicating O^- as the reactive site. Large near-degeneracy effects (20 kcal/mol) make at least a multiconfiguration SCF treatment necessary to compute the barrier heights.

Introduction

The conversion of methane into higher carbon derivatives has attracted a large amount of experimental attention over the past few years. The possibility of converting the relatively abundant methane component of natural gas into products more easily transported and used for synthesis has a large economic potential.[1] Many different potential catalysts have been developed and tested to this end. Among the most promising so far are different alkali-doped metal oxides, such as Li/Sm_2O_3, Na/CaO, and Li/MgO, or mixed oxides, such as $LiNiO_2$.

At high partial pressures of methane, gas-phase oxidation of methane with O_2 to give C/C coupled products, such as C_2H_6, C_2H_4, and higher alkanes, proceeds with high selectivity and conversion rate at temperatures above 500 °C.[2] The reaction proceeds as a gas-phase radical chain reaction with selectivity increasing with temperature. At these high pressures solid catalysts, such as Li/MgO, actually inhibit the reaction, presumably through radical chain termination at the surface.[2] At low methane partial pressures the catalyst is required, however, to give acceptable conversion rates and selectivity.

MgO has been shown to activate methane also without doping and at low temperatures.[3,4] In these experiments the MgO was pretreated at high temperatures before being cooled to 77 K and the formation of different absorption sites of hydrogen and methane was studied by temperature-programmed desorption techniques. The results indicate that in this case[3] low-coordinated ions at steps or crystal imperfections are responsible for the observed decomposition of methane. Using thermally decomposed N_2O as oxidant in the reaction over MgO results in an O_2^- surface species,[4] which was proposed to be the active species, while photodecomposition of N_2O resulted in the formation of O^- at the surface as seen from ESR measurements. When N_2O was used as oxidant in this study, no indication of activity of low-coordinated ions was found.

When methane is passed over MgO at temperatures above approximately 800 K, CH_3 radicals are formed, which are released into the gas phase and may be collected in an argon matrix[5,6] or trapped in a tandem reactor.[7] Thus the abstraction of hydrogen from CH_4 is experimentally verified. Furthermore, in the work of Driscoll et al.,[5] a strong correlation between the activity of the surface (measured in terms of the amount of radicals produced) and the concentration of surface O^- species was found. In the case of the undoped MgO surface these O^- radical ions were suggested to be formed from O_2 at intrinsic cation vacancies. Doping with Li results in a higher concentration of O^- at the surface and a strong increase in reactivity.

The rate-determining step in the conversion of methane to higher derivatives has been shown to be the abstraction of hydrogen at the surface.[5,8] The reactivity of the surface is strongly dependent on the concentration of O^- centers, which may be created by doping with Li as in the case of Li/MgO,[5-10] Li/SmO_2O_3,[10] and Li/NiO.[11] The activity of a dopant is furthermore dependent on size and possibility of entering the surface. Thus, Li/MgO and Na/CaO are reactive, while Na/MgO is not.[9]

The picture emerging from the experimental investigations is thus one where the active centers consist mainly of O^- species at the surface formed either by doping with alkali metals or by decomposition of O_2 over cation vacancies. Steps and dislocations with lower coordination of the anion may also contribute to the activity. The initial reaction step is the abstraction of a hydrogen atom from methane over an O^- site and the formation of a methyl radical and a surface OH^- group.

Theoretical studies of the hydrogen abstraction from methane over oxide catalysts have been performed by Anderson and coworkers[12] using a cluster model and a parametrized computational approach. In their work on methane conversion over an MoO_3 catalyst,[13] O^- was found to activate the C–H bond with an activation energy of 16 kcal/mol. For the corresponding methane conversion over a model of Li-doped MgO, they reported[14] a zero activation energy barrier for the reaction with O^- and a rather strong tendency of the resulting methyl radical to associate to the surface; their reported binding energies to Mg^{2+} at face, edge, and corner sites are in the range 1–1.5 eV. Very recently Zichovic-Wilson et al.[15] reported on an unrestricted Hartree–Fock study of oxidative coupling of methane on MgO. Though their method does not contain an empirical parameters, the model of the surface that they employ is clearly insufficient: a linear O–Mg–O cluster terminated by unit charge pseudo-atoms. No

† Current address: Dept. of Chemistry, University of Bergen, Allegt 41, N-5007 Bergen, Norway.

(1) Jones, C. A.; Leonard, J. J.; Sofranko, J. A. *Energy Fuels* **1987**, *1*, 12.
(2) Onsager, O. T.; Lødeng, R.; Søraker, P.; Anundskaas, A.; Helleborg, B. *Catal. Today* **1989**, *4*, 355.
(3) Ito, T.; Tashiro, T.; Watanabe, T.; Toi, K.; Ikemoto, I. *Chem. Lett.* **1987**, 1723.
(4) Tashiro, T.; Ito, T.; Toi, K. *J. Chem. Soc., Faraday Trans.* **1990**, *86*, 1139.
(5) Driscoll, D. J.; Martir, W.; Wang, J.-X.; Lunsford, J. H. *J. Am. Chem. Soc.* **1985**, *107*, 58.
(6) Driscoll, D. J.; Lunsford, J. H. *J. Phys. Chem.* **1985**, *89*, 4415.
(7) Amorebieta, V. T.; Colussi, A. J. *J. Phys. Chem.* **1988**, *92*, 4576.
(8) Cant, N. W.; Lukey, C. A.; Nelson, P. F.; Tyler, R. J. *J. Chem. Soc., Chem. Commun.* **1988**, 766.
(9) Lin, C.-H.; Ito, T.; Wang, J.-X.; Lunsford, J. H. *J. Am. Chem. Soc.* **1987**, *109*, 4808.
(10) Hutchings, G. J.; Woodhouse, J. R.; Scurrell, M. S. *J. Chem. Soc., Faraday Trans. 1* **1989**, *85*, 2507.
(11) Badyal, J. P. S.; Zhang, X.; Lambert, R. M. *Surf. Sci. Lett.* **1990**, *225*, L15.
(12) Yu, J.; Anderson, A. B. *J. Am. Chem. Soc.* **1990**, *112*, 7218, and references therein.
(13) Mehandru, S. P.; Anderson, A. B.; Brazdil, J. F.; Grasselli, R. K. *J. Phys. Chem.* **1987**, *91*, 2930.
(14) Mehandru, S. P.; Anderson, A. B.; Brazdil, J. F. *J. Am. Chem. Soc.* **1988**, *110*, 1715.
(15) Zicovich-Wilson, C. M.; Gonzalez-Luque, R.; Viruela-Martin, P. M. *J. Mol. Struct. (THEOCHEM)* **1990**, *208*, 153.

0022-3654/91/2095-7401$02.50/0

account was taken of the Madelung potential generated by the surrounding ionic crystal and effects of increasing the cluster size were not investigated. In the present work we will present results from high-level ab initio quantum chemical calculations on the abstraction reaction over a more extended cluster model of the crystal imbedded in the Madelung potential appropriate for the surface. The effects of different types of dopants will also be considered.

We have thus studied the abstraction of hydrogen from methane by computing the interaction between the approaching methane and an M–O species at the surface of the oxide crystal in the appropriate Madelung potential. The metal (M) has been either Mg, as in the surrounding MgO crystal, or one of several dopants (Li, Be, Na, and Al). The effects of the immediate surroundings on the active center have been studied by including the nearest neighbors explicitly in the calculations. Additional studies of the effects of a cation vacancy have been performed by leaving the metal site empty in the cluster model of the system. The reactions at steps and dislocations will be considered in future work.[16] The calculations have been performed at different levels of approximation including MCSCF and multireference CI in order to obtain reliable values for exothermicities and barrier heights. The results clearly indicate that surface O^{2-} is unreactive, while Li and Na doping produce a reactive O^- center in accordance with the experimental results.

Computational Details

The reactions site was modeled by a cluster embedded in a point-charge array, the clusters ranging in size from a single M–O unit to 11 atoms. The reactive oxygen was contained in a perfect crystal structure surface layer, while the number and description of the nearest neighbors in the second and third layers were varied. The four nearest-neighbor magnesium atoms in the surface layer were treated at three different levels of approximation. In the simplest model they were all replaced by +2 point charges. In the second level of approximation they were described by frozen SCF wave functions determined by calculation on a Mg^{2+} ion in a bulk Madelung potential using a large uncontracted (12s 8p) basis set.[17] Only the occupied orbitals were then retained in the calculations by contracting the basis set to minimal basis size by use of the Raffenetti contraction scheme.[18] This significantly reduces the size of the calculations in the case of the methane dissociation over the cluster. In the best description, the Mg^{2+} ions were treated more flexibly with the standard [4s3p] basis as defined in ref 19. The metal atom beneath the central oxygen was always treated at the all-electron level, using basis sets of standard quality. Its four neighboring oxygens in layer 2 and the single nearest oxygen in layer 3 were treated either at the all-electron level by using a [4s 3p] basis or as point charges.

The central reacting oxygen was described by use of the standard [4s 4p 1d] basis from ref 19, where a diffuse p function and a d function have been added to the Dunning [4s 3p] set.[20] For oxygen anions further from the reaction site the [4s 3p] set has been used without extensions. Basis sets for carbon and hydrogen were identical with those used in ref 19. These bases are balanced to describe the bond strengths in the hydroxide radical and methane to similar accuracy. For Li, Mg, and Al we have used the standard bases developed in ref 19, and basis sets of similar quality were used for Na and Be. The two metals with a 2s valence shell were described with the MIDI-3 basis[21] with three extra p functions; Li (α_p = 1.5, 0.6, 0.24) and Be (α_p = 0.32, 0.11, 0.04). For Na and Mg the MIDI-3 sets[21] were used with two extra, diffuse p functions with exponents Na (α_p = 0.11, 0.03) and Mg (α_p = 0.2, 0.05). The standard basis set for Al consists of MINI-4[21] with the most diffuse s function uncontracted, and an additional p and d function; Al (α_p = 0.12, α_d = 0.18). These bases have been shown[19] to give a reasonable description of the metal in gas-phase hydrogen abstraction using metal oxides. In the current systems, the increased ionicity places less demand on the metal bases, and they are certainly of adequate quality.

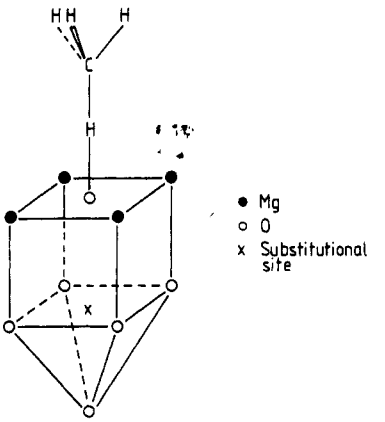

Figure 1. Geometry and structure of three-layer cluster model of the MgO(001) surface with incoming CH_4.

In all calculations the crystal structure was kept unrelaxed and with the experimental Mg–O distance of 2.105 Å.[22] This is very reasonable for a perfect (001) surface, in which case the rumpling and dilatation have been calculated to be 2% and 0.7%, respectively.[23] In the case of dopants, the doping metal was assumed to stay on-center at an Mg^{2+} site.

The calculations have been performed at the SCF, CASSCF, and externally contracted multireference CI (CCI)[24] levels of approximation. Optimization of transition-state and final-state structures has been done at the CASSCF level using pointwise calculations. The barrier heights and exothermicities were then determined at the CCI level using the computed CASSCF geometries. The Davidson correction (+Q)[25] for higher excitations has been included in all reported CCI energies. In all the CASSCF calculations the bonds to be formed or broken were correlated, i.e., the C–H and the O–H bonds. In addition, the strongly occupied metal valence orbitals of cations with changing covalency to the central oxygen were included in the active space. Finally, correlation of the reactive oxygen π-like lone pairs was included to improve the electron affinity of oxygen. In the CCI all configurations from the CASSCF wave function with a coefficient larger than 0.05 were taken as reference. In the correlated treatment the O (2s) lone pair was included, as well as all electrons from the CASSCF active space.

The reactions were assumed to proceed with the transferred hydrogen, the receiving oxygen, and the methane carbon in a collinear configuration (Figure 1), and the methyl group was assumed to maintain C_{3v} symmetry throughout the reaction. Since the C–H bond distances in CH_4 and in the CH_3 radical are very similar these were kept fixed, and the remaining geometry parameters to optimize for the transition state become the O–H and H–C distances and the umbrella angle of the H–CH_3 moiety. The structures were optimized in a two-step procedure with first a two-dimensional grid optimization of O–H and H–C for fixed angle followed by an optimization of the angle at the optimized geometry. The distances were then reoptimized for the optimal angle.

When a cluster model is used to describe an ionic crystal locally, it is important to include the long-range forces on the cluster from the remaining part of the crystal. We approximate the resulting

(16) Børve, K. J., to be published.
(17) Åkeby, H.; Pettersson, L. G. M. *Chem. Phys. Lett.* **1988**, *146*, 511.
(18) Raffenetti, R. C. *J. Chem. Phys.* **1973**, *58*, 4452.
(19) Børve, K. J.; Pettersson, L. G. M. *J. Phys. Chem.* **1991**, *95*, 3214.
(20) Dunning, T. H. *J. Chem. Phys.* **1970**, *53*, 2823.
(21) Tatewaki, H.; Huzinaga, S. *J. Comput. Chem.* **1990**, *1*, 205.
(22) Wyckoff, R. W. G. *Crystal Structures*, 2nd ed.; Interscience Publishers: New York, 1965; Vol. 1.
(23) Pope, S. A.; Guest, M. F.; Hillier, I. H.; Colbourn, E. A.; Mackrodt, W. C.; Kendrick, J. *Phys. Rev. B* **1983**, *28*, 2191.
(24) Siegbahn, P. E. M. *Int. J. Quantum Chem.* **1983**, *23*, 1869.
(25) Davidson, E. R. In *The World of Quantum Chemistry*; Daudel, R., Pullmann, B., Eds.; Reidel: Dordrecht, The Netherlands, 1974. Blomberg, M. R. A.; Siegbahn, P. E. M. *J. Chem. Phys.* **1982**, *78*, 5682.

potential with its leading term, i.e., the Madelung potential

$$V(\vec{r}) = \sum_i \sum_{hkl} \frac{q_i}{|\vec{r} - \vec{r}_{hkl} - \vec{r}_i|}$$

where the ions are represented by point charges at the equilibrium geometries of the ions. The sum runs over ions in a unit cell (index i) and over lattice points (indices hkl). It is well-known that this sum is conditionally convergent and a balanced summation is required to obtain the physically correct value. For an infinite crystal this is a long-solved problem, and many of the algorithms currently in use are modifications of Ewalds method.[26] The rapidly varying contribution to the Madelung potential from the nearest point charges is summed in direct space, whereas the slowly varying potential from the more distant ions is summed in reciprocal space, where it is expressed accurately on a small $\vec{k}$ domain. This separation is achieved by multiplying each Coulomb term with $1 \equiv \text{erf}(Gr) + \text{erfc}(Gr)$, where G is an adjustable parameter to increase convergence speed and r is the radial distance from the ion site in question.

The introduction of a surface removes the periodicity in the direction normal to the surface (z direction, say), but the remaining two-dimensional periodicity may be utilized[27] in a manner similar to that of Ewald. Summation in the z direction has to be performed in direct space; this amounts to summing over sheets of ions parallel to the surface plane. The surface Madelung potential is very rapidly convergent with the number of ion sheets that are added; typically only three to six layers are needed to converge the potential at the surface to five decimals.

Having calculated the potential on a grid enclosing the chosen cluster, we expand the Madelung potential in a second, finite array of point charges. The ions are positioned at the original ion sites, but the charges are determined in a least-squares manner to reproduce the correct surface Madelung potential. A single variable charge is assigned to each group of symmetry-related ions, and an additional constraint of overall charge neutrality is imposed. This representation of the Madelung potential facilitates the use of standard integral packages in the evaluation of matrix elements. Typically, the relative error resulting from expanding the Madelung potential in point charges was found to be less than 0.1%. The properties that are of interest in this study are insensitive to the detailed form of the potential, and no appreciable error in the energetics is expected to result from the point-charge expansion.

Results and Discussion

We have recently studied[19] the gas-phase hydrogen abstraction reactions of CH_4 with LiO, MgO, and AlO and we will begin this section with a short summary of the results obtained in that study. For these three (gas-phase) metal oxides the charge on the oxygen is close to one extra electron. For Li the interaction with oxygen is completely ionic, while for both Mg and Al the resulting bonding has both ionic and covalent contributions. All three reactions are exothermic with computed values of 14, 8, and 6 kcal/mol for LiO, MgO, and AlO, respectively. The barriers to the abstraction reaction were computed to be 13, 11, and 16 kcal/mol given in the same order as above.[19] In the case of diatomic, gas-phase LiO the ground state is the X $^2\Pi$ state, which has a $\sigma^2\pi^3$ valence occupation, which thus has an open π shell giving a favorable interaction with methane approaching at 90° to the Li–O bond. However, this leads to an unfavorable 90° bent Li–OH final state. For the collinear approach, a $\sigma \rightarrow \pi$ excitation resulting in a $\sigma^1\pi^4$ valence occupation is required to give a favorable overlap with an approaching hydrogen in CH_4. This corresponds to the lowest excited, A $^2\Sigma^+$, state of the diatomic LiO molecule. In the gas phase these two states are separated by close to 7 kcal/mol as obtained in ref 19. The balance between the unfavorable final state for the 90° approach and the need to involve an excited molecular state in the collinear approach leads to very similar barriers independent of angle of approach. By exciting the LiO molecule to the A $^2\Sigma^+$ state before the reaction, the barrier will thus be reduced to 6 kcal/mol for the gas-phase reaction.

TABLE I: Computed Hydrogen Affinities E^H_{MO} (kcal/mol) for Different Metal Substituents in Layer 2[a]

	SCF	CASSCF	CCI+Q
	Madelung Potential		
Li	77	107	107
Be	3	−4	8
Na	77	106	106
Mg	14	8	20
Al			27
	Frozen Nearest Neighbors and Madelung Potential		
Li	73	102	
Mg	−15	−21	

[a] The surrounding crystal is represented by its Madelung potential only or by the frozen wave functions of the four nearest Mg^{2+} neighbors to the oxygen ion in addition to the Madelung potential.

When LiO is considered as a substitution or dopant in the Madelung potential from the extended MgO crystal with oxygen in the surface layer, the splitting between the two low-lying states of LiO changes. The molecular $\sigma^1\pi^4$ ($^2\Sigma^+$) state becomes the lowest state with a CASSCF energy difference of close to 43 kcal/mol to the $^2\Pi$ molecular state. The π^4 occupation results in a larger charge density close to the surrounding positive counterions in the plane than does the π^3 occupation. This then places the open shell pointing out of the surface and results in a reactivity toward approaching CH_4 corresponding to that of the gas-phase diatomic LiO $^2\Sigma^+$ state.

The surrounding counterions in the crystal tend to stabilize the more ionic components in the wave functions. In the case of LiO the charge transfer is already complete for the gas-phase system and no further charge transfer is possible. The inclusion of the potential from the remaining crystal then has a significant effect on the relative stabilities of the two states, but not on the resulting reactivities. For both MgO and AlO additional charge is moved over to the oxygen, however, resulting in a charge distribution close to $M^{2+}O^{2-}$. Changing the charge state of oxygen from O^- to O^{2-} changes the electronic structure from a radical-like valence shell on O to a closed shell, which strongly reduces the reactivity.

To obtain an estimate of the exothermicities of the reactions with the different substituents and with the undoped MgO(001) surface we may consider the respective hydrogen affinities as computed in the surrounding surface-layer Madelung potential. The hydrogen affinity may be computed as $E^H_{MO} = E_{MO} + E_H - E_{MOH}$ where E_X is the total energy of the metal oxide (MO), hydrogen (H), or metal hydroxide (MOH) (Table I). The C–H bond strength, D_e, computed at the single-reference CCI+Q level by using the present basis sets and with eight electrons correlated is 107 kcal/mol.[19] Only Li and Na as substituents are able to compensate the energy loss resulting from the C–H bond breaking by a comparable gain in energy from formation of the surface hydroxide species in the field of the remaining crystal. Mg, Be and Al as second-layer cations all result in hydrogen affinities of less than 30 kcal/mol and thus endothermic reactions requiring more than 70 kcal/mol to reach the products.

The model for computing the hydrogen affinity was further improved by surrounding the surface oxygen ion by its four nearest Mg^{2+} neighbors with wave functions frozen either from calculations on the ions or from the ions in the Madelung potential. This had no effect on the hydrogen affinity with Li as a substituent and further reduced the affinity of Mg–O for hydrogen to give a resulting negative affinity. Thus the calculations using only the Madelung potential provide a reliable measure in this case for selecting systems for further study. The hydrogen affinities of the Mg, Be, and Al dopants are clearly too low for these systems to be of interest in the hydrogen abstraction reaction. Thus, these metals will not be further considered in the present work.

The difference in energy between the two states of diatomic LiO is more strongly affected by the replacement of the nearest-neighbor point charges in the first layer by Mg^{2+} ions; the energy difference is reduced from 43 (CASSCF) to 24 kcal/mol

(26) Ewald, P. P. *Ann. Phys.* (*Leipzig*) **1921**, *64*, 253.
(27) Parry, D. E. *Surf. Sci.* **1975**, *49*, 433. Parry, D. E. *Surf. Sci.* **1976**, *54*, 195.

TABLE II: Results for the Abstraction Reaction, $MO_{embed} + HCH_3 \rightarrow MOH_{embed} + {}^{\bullet}CH_3$[a]

	SCF	CASSCF	CCI+Q
	Exothermicity ($-\Delta E$)		
LiO	-9.2	10.2	3.3 (0.3)
LiO (Mg_4O_5)	-8.5	10.6	3.9 (0.9)
NaO	-10.0	9.6	1.7 (-1.3)
Mg vacancy (Mg_4O_5)	-15.5	-11.4	-5.2 (-8.2)
Mg^+ vacancy (Mg_4O_5)	-16.5		-7.3 (-10.3)
	Barrier Height (E^*)		
LiO (gas-phase TS)	24.6	7.1	4.8
LiO (reopt TS)		6.2	4.3
LiO (Mg_4O_5)	26.0	8.2	6.3
NaO	25.6	5.0	4.2
Mg vacancy (Mg_4O_5)	23.4	17.5	10.5
Mg^+ vacancy (Mg_4O_5)	19.3	14.1	6.4
	$E_{TS} - E_{Prod}$		
LiO (gas-phase TS)	15.4	17.3	8.1
LiO (reopt TS)		16.4	7.6
LiO (Mg_4O_5)	17.4	18.8	10.2
NaO	15.6	14.6	5.9
Mg vacancy (Mg_4O_5)	7.9	6.1	5.3
Mg^+ vacancy (Mg_4O_5)	2.8		-0.9
	Transition-State Geometry		
LiO(g)	1.35	1.21	107
LiO (MgO)	1.37	1.27	105

[a] All energies in kilocalories per mole and distances in angstroms. Values in parentheses include a correction for the effect of correlating all C–H bonds (see text).

due to the Pauli repulsion with the surrounding ions. The reactive $^2\Sigma^+$ molecular state is still the lowest by a substantial amount, however.

The interesting dopant ions are thus Li^+ and Na^+, and the reactions of the surface doped with these ions will now be considered in more detail. The first model will be to simply insert LiO or NaO in the Madelung field from the remaining crystal with the metal in the second layer and the oxygen at the surface. This will then be extended to include the four nearest-neighbor Mg–O units and the third-layer O^{2-} immediately beneath Li or Na. The Mg^{2+} ion cores were kept frozen while the wave function for the remaining parts of the system was optimized in a completely variational treatment. The M–O (Mg_4O_5) cluster was then placed in the appropriate Madelung crystal field. This treatment allows charge to relax fully (except for unimportant polarization effects on the Mg^{2+} ion cores) and allows the different subunits of the system to assume the most favorable charge state.

The exothermicities of the Li and Na reactions, in the Madelung field only, are obtained from Table I by subtracting the computed C–H binding energy (D_e) of methane, 107 kcal/mol.[19] The resulting values at the CCI+Q level then become close to zero for the reactions of both Li and Na. Zero-point vibrations have not been included in this estimate, but are expected to increase the computed exothermicities somewhat. Surrounding the M–O center by the nearest-neighbor cluster does not affect the computed exothermicity for LiO (Table II) and is not expected to have an appreciable effect on the NaO reaction. It should be noted in connection with the computed exothermicities in Table II that the computed C–H bond strength with all bonds correlated (eight electrons) is 3 kcal/mol larger than when only the C–H bond to be broken is correlated. In the calculations on the combined system, the M–O and one C–H bond were correlated and thus we have added a correction for the underestimate of the C–H bond strength to the computed exothermicities (values in parentheses).

The transition-state structure for the reaction between gas-phase LiO and methane has been reported earlier, but is included for easy comparison in Table II, LiO(g). Computing the barrier height for this structure and with the Madelung field only, we find a low value (CCI+Q) of 4.8 kcal/mol. Reoptimization of the transition-state structure in the field of the crystal results in only minor differences and a slight lowering of the barrier by 0.5 kcal/mol to 4.3 kcal/mol. Embedding the LiO center in the Mg_4O_5 cluster again results in only minor effects on the barrier height and the resulting low barrier of 6 kcal/mol is in good accord with the observed reactivity of Li-doped MgO. The abstraction reaction proceeds by the formation of a three-center two-electron σ bond between the oxygen, hydrogen, and carbon centers. This transforms into the O–H bond in the surface hydroxide group. Simultaneously the O^- radical character shifts over toward the methyl group. The barrier for the reaction with Na as dopant was then computed in the Madelung field by using the same transition-state geometry as optimized for LiO in the field. The resulting barrier is identical with that obtained for the LiO system, showing that the reaction is determined mainly by the O^- with Li^+ and Na^+ as equivalent stabilizing counterions. Experimentally, however, doping MgO with Na has been observed to have a much smaller effect on the measured reactivity.[5,9] This has been explained as due to the different sizes of the Li^+ and Na^+ counterions, where Na^+ because of its larger size would not be possible to incorporate into the crystal lattice.[5] The present results support this view, since Li and Na incorporated in the lattice should show the same reactivities. CaO and MgO have the same crystal structures, but different lattice parameters: 4.21 and 4.81 Å for MgO and CaO,[22] respectively. Thus, in the case of CaO, an Na dopant should stabilize the reactive species O^- in the same manner as Li or Na in MgO. Considering the relative ionic sizes, Na^+ and Li^+ should both fit into the CaO lattice at substitutional sites and both Na and Li doping of CaO should result in similar reactivities, as is also observed experimentally.[9]

The association of the methyl radical to the surface was investigated by computing the interaction between the radical and both Mg^{2+} and O^{2-} sites at the surface. Mehandru et al.[14] found the methyl radical bound to Mg^{2+} by 1–1.5 eV depending on the site studied. In the present work, however, the interaction is found to be repulsive. This is the case both for association to an Mg^{2+} site and to an O^{2-} ion. Thus, for the perfect crystal sites investigated in the present work the hydrogen abstraction would lead to a gas-phase methyl radical.

The large difference between the barrier heights at the SCF and CASSCF levels shows the importance of near-degeneracy effects for the transition-state wave function. The effect of dynamical correlation as measured from the difference between the CASSCF and CCI+Q results is much smaller in this case and only of the order of a few kilocalories per mole. This again underlines the well-known importance of a multiconfigurational description of bond-breaking processes.

Experimentally, undoped MgO crystals are also found to react with CH_4, producing gas-phase methyl radicals.[5-7] It has been suggested that also in this case O^- centers are reponsible for the reactivity[5] now associated with cation vacancies in the lattice. Another suggestion has been a high activity connected with low-coordinated ions at steps and imperfections in the lattice.[3] This possibility will be investigated in future work,[16] and here we will focus our interest on the reactivity of oxygen ions above a cation vacancy in the first MgO(001) subsurface layer.

The cluster model chosen to describe the cation vacancy has the top oxygen site occupied and surrounded by its four nearest-neighbor MgO units. Two different basis set descriptions have been used for the surface oxygen: either a smaller [4s 3p] basis or the more extended standard [4s 4p 1d] basis set used in studying the effects of doping (above). The Mg^{2+} ions have furthermore been treated at two different levels of approximation, where the first is to simply include them as frozen atomic ions and the second to also allow a complete relaxation of the orbitals associated with these ions. Finally, the bottom oxygen was also included, either as a -2 point charge or as an all-electron O^{2-} ion. The cluster was always embedded in the appropriate Madelung field from the remaining crystal.

Three different charge states of the removed Mg atom have been considered (Table III): Mg^{2+}, Mg^+, and neutral Mg. This nomenclature does not refer to a physically removed ion, but rather is used to specify the total charge on the remaining cluster assuming an originally completely ionic $Mg^{2+}O^{2-}$ charge distribution. In particular, the charge localized near the vacancy affects the

TABLE III: Mg Vacancy in the Second Surface Layer[a]

vacancy	O(3)[b]	hydrogen affinity (E^H) SCF	CASSCF	CCI+Q
Mg^{2+}	AE	35.7		
Mg^{+}	AE	59.3	88.6	90.8
Mg^{0}	AE	62.8	91.8	94.0
Mg^{+}	PC	58.9	88.2	90.5
Mg^{+}[c]	PC	65.2	95.0	96.1
Mg^{+}[c,d]	PC	70.6		97.0
Mg^{0}[c,d]	AE	71.7	85.3	99.2

[a] All energies are in kilocalories per mole. [b] Description in third-layer (bottom) oxygen where AE indicates all-electron [4s 3p] basis on bottom oxygen and PC a point-charge representation of O^{2-}. [c] [4s 4p 1d] basis on the top O. [d] Frozen orbitals on Mg^{2+}.

charge on the topmost, reactive oxygen. As a qualitative initial investigation, all three systems were studied by using the smaller basis set description of the oxygen atoms and with the magnesium atoms fully relaxed. When Mg^{2+} is removed, the topmost oxygen remains doubly charged with a closed valence shell character and a low hydrogen affinity, E^H. This system is unreactive and will not be considered further. Upon removal of singly charged or neutral Mg a quite different picture is obtained; in both cases the reactive surface oxygen becomes close to O^- with the open-shell orbital pointing out of the surface. The resulting hydrogen affinity then becomes similar to that found in the case of alkali-metal doping.

For the Mg^+ vacancy the open shell is strongly located on the surface oxygen, as seen also from the negligible effect on the hydrogen affinity from replacing the bottom oxygen by a −2 point charge. The Mg^0 vacancy, on the other hand, is best described as a biradical state with open shells on both the top and bottom oxygens. The interaction between the open shells is very small; the triplet-coupled SCF solution and a two-configuration description of the singlet state are degenerate.

In order to study the dissociation process of methane, a more compact description of the Mg^{2+} ions, based on frozen ionic cores, was used. The approximation to freeze the surrounding ionic Mg^{2+} cores has a very small effect on the results; in the case of the Mg^{2+} vacancy, the hydrogen affinity is increased by less than 1 kcal/mol. Our final results for the hydrogen affinities of the Mg^+ and Mg^0 vacancies and the corresponding reaction barriers were then obtained from the larger [4s 4p 1d] basis set for the reactive oxygen and with frozen Mg^{2+} nearest neighbors. The E^H is increased by 5–6 kcal/mol from the improved description of the top oxygen. The resulting exothermicities (Table II) become slightly negative and the computed barriers for hydrogen abstraction ($E^‡$) are very similar to those found for the Li and Na doped systems. For the case of an Mg^0 vacancy, $\Delta E > E^‡$, i.e., it may be that this reaction has no transition state.

Conclusions

The charge state of oxygen in the perfect MgO(001) crystal is best represented as O^{2-}. This is a closed-shell ion with a very low affinity for hydrogen; abstraction of hydrogen from methane at this site is very unfavorable and requires more than 70 kcal/mol. Dopants, such as Al or Be, also provide enough electrons to the oxygen to give an unreactive O^{2-} species while doping with alkali metals, such as Li or Na, result in an O^- surface species that exhibits a low barrier to hydrogen abstraction. A similar charge state of oxygen and subsequent reactivity may also be found over a cation vacancy.

Acknowledgment. Financial support from the Norwegian Research Council for Science and the Humanities is gratefully acknowledged for K.J.B.

Registry No. CH_4, 74-82-8; MgO, 1039-48-1; Li, 7439-93-2; Na, 7440-23-5; Be, 7440-41-7; Al, 7429-90-5; LiO, 12142-77-7; NaO, 12401-86-4.

Quantitative ^{95}Mo Liquid NMR Study of the Adsorption of Oxomolybdate Species on γ-Al_2O_3

P. Sarrazin,[†,‡] B. Mouchel,[§] and S. Kasztelan*[,†,‡]

Laboratoire de Catalyse Hétérogène et Homogène, UA CNRS 402, and Centre Commun de Résonance Magnétique Nucléaire, Université des Sciences et Techniques de Lille Flandres-Artois, F-59655 Villeneuve d'Ascq, Cedex, France *(Received: October 31, 1990)*

^{95}Mo NMR has been quantitatively used to investigate the adsorption of oxomolybdate species inside the pore volume of a γ-alumina support. The results show that a large amount (more than 97% in this study) of the molybdenum contained in the initial solution is fixed by the alumina support during the impregnation step. This strong adsorption has been observed for a large range of Mo concentrations. The nature of the Mo species not adsorbed is the molybdate ion, and it is shown that the heptamolybdate anion, initially present in solution is preferentially adsorbed. This result suggests that the buffer effect of the alumina is not strong enough to decompose the heptamolybdate ion into molybdate. Impregnations of γ-alumina with Mo solutions at different pH values lead to noticeable differences in the adsorption capacity of the support. The nature of the interaction between the anion and the alumina adsorption sites is proposed to be electrostatic. The so-called monolayer coverage of γ-alumina is proposed to result from the saturation by heptamolybdate anions of a number of adsorption sites estimated at 0.7 site/nm^2 of BET area for the γ-alumina used.

Introduction

Impregnation is a process commonly used for the deposition of metal salts on an oxide support. One of the major methods of impregnation used, so-called incipient wetness, involves the filling of the pore volume of a porous support by a solution containing the metal salt to be deposited. It is important to get a better knowledge of the phenomenon occurring inside the pores of a high surface area support during the impregnation step to be able to generate catalysts containing well-defined species with monitored repartition of these species on the support surface.

The investigation of this phenomenon is in general limited by the lack of characterization techniques able to probe the solution inside the pores of the support. Thus, in the case of supported molybdenum catalysts, of wide importance in the field of catalysis,

*To whom correspondence should be addressed.
† Laboratoire de Catalyse Hétérogène et Homogène.
‡ Present address: Institut Français du Pétrole, B.P. 311, 92506 Rueil-Malmaison, Cedex, France.
§ Centre Commun de Résonance Magnétique Nucléaire.

0022-3654/91/2095-7405$02.50/0